PAPER

Check for updates

A highly sensitive and selective chemosensor for Pb²⁺ based on quinoline–coumarin†

Xianjiao Meng,[a] Duanlin Cao,[a] Zhiyong Hu,[ab] Xinghua Han,[ab] Zhichun Li[a] and Wenbing Ma (iD) *[ab]

In this study, a highly sensitive and selective fluorescent chemosensor, ethyl(*E*)-2-((2-((2-(7-(diethylamino)-2-oxo-2*H*-chromene-3-carbonyl)hydrazono)methyl)quinolin-8-yl)oxy)acetate (**1**), was synthesized and characterized by ¹H NMR, ¹³C NMR and ESI-MS. Sensor **1** showed an "on−off" fluorescence response to Pb²⁺ with a 1 : 1 binding stoichiometry in CH₃CN/HEPES buffer medium (9 : 1 v/v). The detection limit of sensor **1** to Pb²⁺ was determined to be 0.5 μM, and the stable pH range for Pb²⁺ detection was from 4 to 8.

Introduction

The highly sensitive and selective fluorescent chemosensors for "naked eye" detection of heavy transition metal ions have received considerable attention in recent years.[1–4] Pb²⁺ as an important transition element plays an essential role in various fields.[5] The maximum contaminant level of Pb²⁺ ions in drinking water is set to 10 μg L⁻¹,[6] and exposure to excessive lead can cause mental retardation, muscle paralysis, and memory loss, particularly in children. For this reason, much effort has been made to develop effective methods for Pb²⁺ detection, including ICP-OES (inductively coupled plasma optical emission spectrometry),[7] ICP-MS(inductively coupled plasma mass spectrometry),[8] AFS (atomic fluorescent spectrometry)[9] and AAS (atomic absorption spectrometry),[10] and are capable of the multiple and quantitative determination of Pb²⁺ ion, however, the application of these conventional instrument-based detection methods can be hampered by the need for sophisticated instruments, and complex sampling designs and data analysis; whereas fluorescent chemosensors[11–14] appear to be more effective at Pb²⁺ detection due to their high selectivity and sensitivity.

Although many fluorescence chemosensors have been shown to be capable of identifying Pb²⁺/Ag⁺,[15] Pb²⁺/Fe³⁺/Hg²⁺,[16] and Pb²⁺/Hg²⁺/Cd²⁺,[17] they may show poor binding selectivity for Pb²⁺ over other heavy transition metal ions, which would decrease the accuracy of Pb²⁺ detection in practical applications.[18] Thus, there is a practical need to develop highly sensitive and selective fluorescent chemosensors for naked eye detection of Pb²⁺.[19–23]

8-Hydroxyquinoline-based derivatives have been widely used as fluorescent chemosensors due to their strong coordination ability with metal ions.[24–26] However, these fluorescent chemosensors often exhibit enhanced fluorescence signals in the detection of metal ions due to their weaker fluorescence. Attempts have been made to introduce coumarin-based derivatives as strong fluorescent groups in order to expand the application of 8-hydroxyquinoline.[27–29]

In this study, we reported a novel, highly sensitive and selective fluorescent chemosensor **1** with coumarin as the fluorescence group and C=N bond and quinoline as the identification group for the detection of Pb²⁺. The introduction of hydroxyl into the flexible chain resulted in an improvement of the stability and the selectivity of metal ions. The results showed that sensor **1** showed higher selectivity and sensitivity toward Pb²⁺ over many other metal ions in CH₃CN/HEPES buffer medium (9 : 1 v/v, pH = 7.4).

Experimental

Materials and methods

Other solvents and starting materials were purchased from Aladdin and Energy Chemical Reagents Ltd., (Shanghai, China). Ultrapure water was used in all experiments. The melting points of intermediate and sensor **1** were measured on a WRS-C1 digital melting-point apparatus (Shanghai, China). The pH of all solutions was adjusted on a PHS-3C pH meter (Shanghai, China). The ¹H NMR (400 MHz) and ¹³C NMR (100 MHz) spectra were recorded on a Bruker AVANCE III spectrometer (Switzerland) in CDCl₃ solution. The SEI-MS spectra of intermediate and sensor **1** were recorded on a Bruker Solarix XR Fourier transform-ion cyclotron resonance (FT-ICR) mass spectrometer. The UV-spectra were recorded on a UV-2602 spectrophotometer (Shanghai, China), and the fluorescence spectra were recorded on a HITACHIF-2500 spectrophotometer (Japan).

[a]*School of Chemical Engineering and Technology, North University of China, Taiyuan 030051, P. R. China. E-mail: mawenbing@nuc.edu.cn*

[b]*National Demonstration Center for Experimental Comprehensive Chemical Engineering Education, North University of China, Taiyuan 030051, P. R. China*

Synthesis

Preparation of 2 and 3. As described in a previous study,[30] 8-hydroxyquinaldine (1.6 g, 10.05 mmol), ethyl bromoacetate (1.6 g, 9.58 mmol) and K_2CO_3 (5 g, 36.18 mmol) were dissolved in acetone (20 mL), and then the mixture was heated to reflux for 24 h. After that, the mixture was cooled to room temperature and filtered, and the solvent was removed under reduced pressure. The crude product obtained was purified by column chromatography on silica gel (10% ethyl acetate in petroleum ether), and 1.96 g of white solid **2** was obtained with a 78.5% yield.

Solid **2** (1.5 g, 6 mmol) was dissolved in 1, 4-dioxane (20 mL), and SeO_2 (0.75 g, 6.8 mmol) was added at 65 °C. The mixture was stirred at 80 °C for 2 h and then cooled to room temperature. The solvent was removed under reduced pressure, and 1.31 g of white crystalline solid **3** was obtained by recrystallization from ethyl acetate/hexane (10 mL, 1 : 1, v/v) with a 87% yield and a melting point of 137.3–137.6 °C.

Preparation of 4 and 5. As described in a previous study,[31] 4-diethylaminosalicylaldehyde (1.93 g, 0.01 mol), diethylmalonate (1.92 g, 0.01 mol), glacial acetic acid (0.1 mL) and piperidine (0.1 mL) were dissolved in absolute ethanol (40 mL) and refluxed for 4 h. The mixture was cooled to room temperature and filtered, and the solvent was removed under reduced pressure. A yellow crystalline solid **4** was obtained by recrystallization from ethanol with a 69% yield and a melting point of 85.9 °C.

Solid **4** (2.02 g, 7 mmol) and hydrazine monohydrate (1.4 mL, 28 mmol) were dissolved in ethanol (20 mL) under argon. The mixture was stirred at reflux temperature for 25 min, and then cooled to yield a large amount of precipitate. The precipitate was filtered, washed thoroughly with cold ethanol to obtain yellow product **5** with a 67.2% yield and a melting point of 171.7–172.5 °C.

Preparation of 1. Under argon, solid **5** (121.14 mg, 0.44 mmol) and solid **3** (111.9 mg, 0.43 mmol) were dissolved in ethanol (6 mL) and refluxed for 8 h. Then, the mixture was cooled to room temperature, filtered, washed with cold ethanol, and dried naturally. The crude product obtained was purified by column chromatography on silica gel (2% methanol in dichloromethane) to obtain orange solid **1** with a 98.6% yield and a melting point of 209.5–209.8 °C. The NMR spectra of sensor **1** were shown in Fig. S1 and S2.† HRMS (ESI): m/z calcd for $C_{28}H_{29}N_4O_6$ $[(M + H)^+]$: 517.2082, found 517.2083 (Fig. S3†).

General procedure for recording fluorescence spectra

All fluorescence spectra were recorded on a HITACHIF 2500 fluorescence spectrometer after the addition of metal ions and anions in CH_3CN/HEPES (9 : 1, v/v) buffer (pH = 7.4), and then the excitation wavelength was determined as 440 nm. Metal ions were prepared from chlorine salts of Fe^{3+}, Al^{3+}, Cu^{2+}, Pb^{2+}, Zn^{2+}, Hg^{2+}, Ca^{2+}, Ba^{2+}, Mg^{2+}, Ag^+, Cs^+, Li^+, K^+ and Na^+.

Results and discussion

Effect of pH

Fig. 1 showed the variation of fluorescence intensity of sensor **1** with pH in the absence and presence of Pb^{2+} ions in CH_3CN/
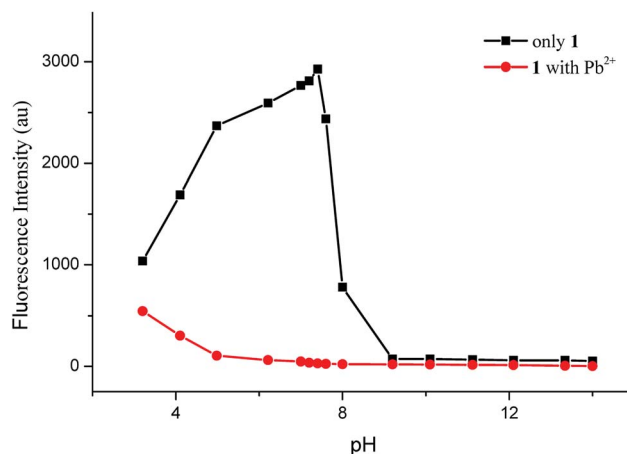

Fig. 1 Variation of fluorescence intensity of sensor **1** (10 μM) in CH_3CN/HEPES buffer medium (9 : 1 v/v, pH = 7.4) with and without Pb^{2+} ions (10 equiv.) with pH at room temperature.

HEPES buffer medium (9 : 1 v/v). The pH was adjusted with 1 N HCl or 1 N NaOH aqueous solution. At pH 3–8, free **1** showed a strong fluorescence, and **1** + Pb^{2+} showed a weak fluorescence; while at pH > 8, free **1** showed a weak fluorescence, because the coumarin lactone ring was converted into hydroxycarboxylate under alkaline conditions. Thus, the stable pH range for Pb^{2+} detection was from 4 to 8, at which free **1** showed stable and strong fluorescence, and fluorescence quenching reached the minimum with the addition of Pb^{2+}.

UV-vis spectral response of sensor 1 to Pb^{2+}

The absorption behavior of probe **1** was investigated by UV-vis spectroscopy in the presence of various metal ions, including Fe^{3+}, Al^{3+}, Cu^{2+}, Pb^{2+}, Zn^{2+}, Hg^{2+}, Ca^{2+}, Ba^{2+}, Mg^{2+}, Ag^+, Cs^+, Li^+, K^+ and Na^+, in CH_3CN/HEPES buffer medium (9 : 1 v/v, pH = 7.4). All absorption spectra showed no remarkable change except that the addition of Pb^{2+} resulted in a red shift of 440 nm to 465 nm and a color change from bright yellow to orange (Fig. 2).

As shown in Fig. 3, the absorption intensity at 440 nm decreased dramatically with the gradual addition of Pb^{2+} up to 20 equiv. into 10 μM sensor **1** in CH_3CN/HEPES buffer medium (9 : 1 v/v, pH = 7.4); whereas that at 465 nm increased gradually with the addition of Pb^{2+}, indicating the formation of **1**–Pb^{2+} complex. In addition, isosbestic points at 451 nm could be clearly observed, thus confirming that probe **1** and **1**–Pb^{2+} complex existed in equilibrium.

Fluorescence responses of sensor 1 to Pb^{2+}

The sensing ability of sensor **1** was investigated by fluorescence experiments in the presence of various metal ions (10 equiv.), including Fe^{3+}, Al^{3+}, Cu^{2+}, Pb^{2+}, Zn^{2+}, Hg^{2+}, Ca^{2+}, Ba^{2+}, Mg^{2+}, Ag^+, Cs^+, Li^+, K^+ and Na^+, in CH_3CN/HEPES buffer medium (9 : 1 v/v, pH = 7.4). The fluorescence spectra were observed at 485 nm (λ_{ex}: 440 nm). Sensor **1** showed a marked fluorescence quenching toward Pb^{2+} compared with other metal ions, resulting in a clear color change from bright yellow to orange. It
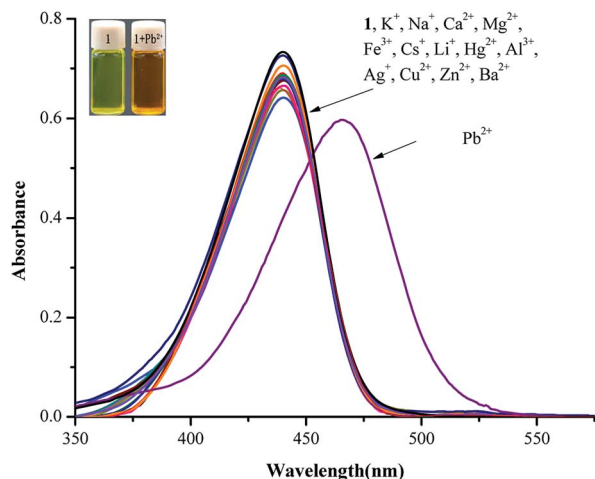
Fig. 2 (a) UV-vis spectra of **1** (10 μM) with the addition of different metal ions (10 equiv.) in CH_3CN/HEPES buffer medium (9 : 1 v/v, pH = 7.4). Inset: the color changed of probe **1** (10 μM) in the absence and presence of Pb^{2+} (20 equiv.).
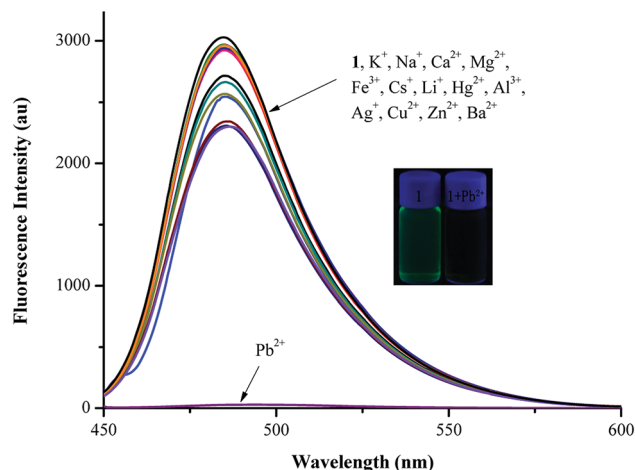

Fig. 4 (a) Fluorescence spectra of sensor **1** (10 μM) with the addition of different metal ions (10 equiv.) in CH_3CN/HEPES buffer medium (9 : 1 v/v, pH = 7.4) with an excitation at 440 nm. Inset: the fluorescence changed of probe **1** (10 μM) in the absence and presence of Pb^{2+} (20 equiv.) under UV light at 365 nm.
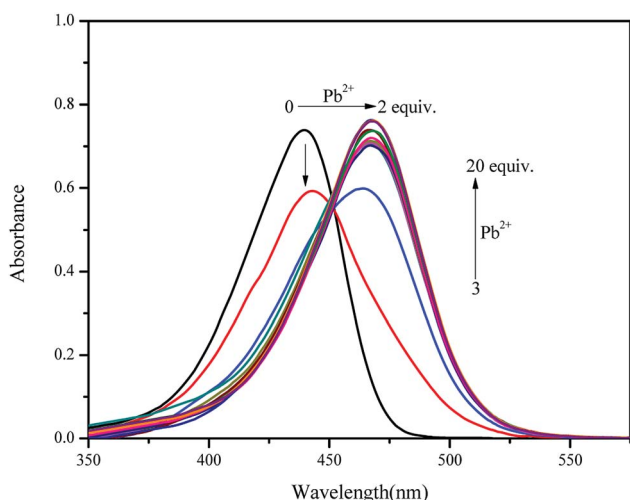

Fig. 3 UV-vis spectra of sensor **1** (10 μM) with the addition of various concentrations [0, 1, 2, 3, 4, 5, 6, 7, 8, 9, 10, 15 and 20 equiv.] of Pb^{2+} in CH_3CN/HEPES buffer medium (9 : 1 v/v, pH = 7.4).
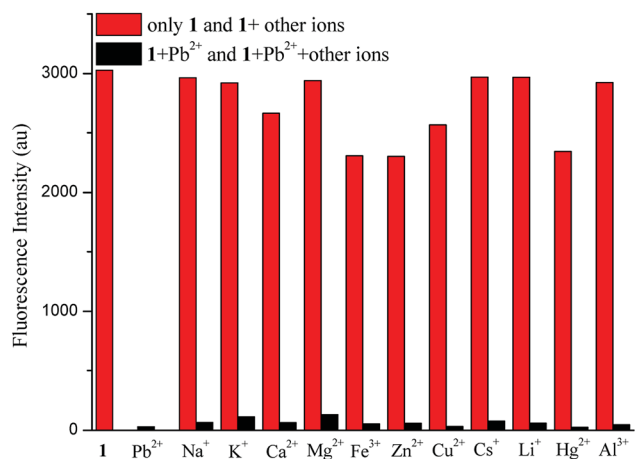

Fig. 5 Fluorescent intensity of sensor **1** (10 μM) with selected cations (10 equiv.) in the absence (red bars) or presence (black bars) of Pb^{2+} (10 equiv.).

also showed a high selectivity for Pb^{2+} and a remarkable fluorescence "turn-off" response (Fig. 4).

Pb^{2+}-selective sensing experiments were performed with 10 μM of sensor **1** in the presence of various metal ions, including Fe^{3+}, Al^{3+}, Cu^{2+}, Zn^{2+}, Hg^{2+}, Ca^{2+}, Ba^{2+}, Mg^{2+}, Ag^+, Cs^+, Li^+, K^+ and Na^+ (10 equiv.), as shown in Fig. 5. Upon the addition of 10 equiv. of Pb^{2+} ions, the solution still showed a distinct fluorescence quenching. All these results suggested that sensor **1** could be used as a chemosensor for selective detection of Pb^{2+} over a wide range of metal ions.

In order to gain further insight into the sensing behavior of sensor **1** to Pb^{2+}, fluorescence titration experiments were performed. Fig. 6 showed that the fluorescence intensity decreased gradually with the increasing concentration of Pb^{2+}. A dramatic fluorescence quenching was observed, and the quenching

efficiency reached a maximum of 99% $[(I_0 - I)/I_0 \times 100\%]$ with the addition of 10 equiv. of Pb^{2+}. The Job plots with fluorescence titrations showed a minimum at about 0.5 mol fractions, indicating that sensor **1** formed a 1 : 1 complex with Pb^{2+} (Scheme 1).

The binding constant K_a was determined to be 2041 M^{-1} (R^2 = 0.9973, Fig. 7). The detection limit was determined to be 0.5 μM according to the formula LOD = $3\sigma/m$, where m was the slope of the linear equation $Y = aX + b$ between fluorescence intensity and concentration (Fig. 8).

The possible mechanism of sensor 1 with Pb^{2+}

The fluorescence quenching efficiency reached a maximum of 99% $[(I_0 - I)/I_0 \times 100\%]$ with the addition of 10 equiv. of Pb^{2+}, and no shift of the emission spectra with increasing Pb^{2+} concentration was observed. This was in good agreement with
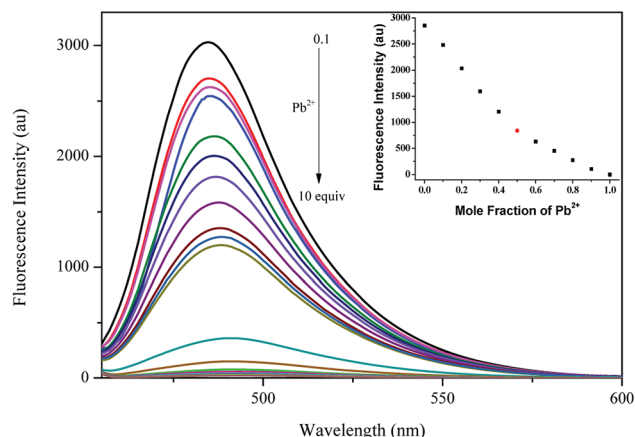
Fig. 6 Fluorescence spectra of sensor **1** (1 μM) with the addition of various concentrations [0, 0.1, 0.2, 0.3, 0.4, 0.5, 0.6, 0.7, 0.8, 0.9, 1.0, 2.0, 3.0, 4.0, 5.0, 6.0, 7.0, 8.0, 9.0 and 10 equiv.] of Pb^{2+} in CH_3CN/HEPES buffer medium (9 : 1 v/v, pH = 7.4) with an excitation at 440 nm. Inset: the Job plots with fluorescence titrations showed an intersection point at about 0.5 mol fractions, indicating that sensor **1** formed a 1 : 1 complex with Pb^{2+}.
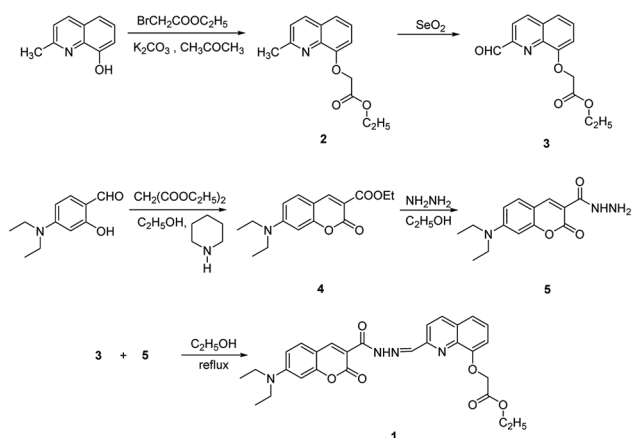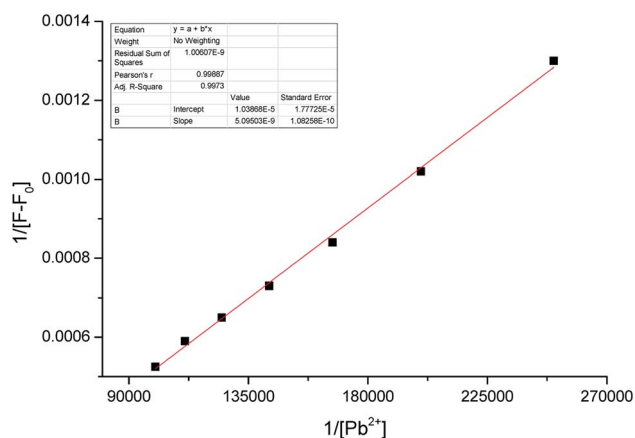

Scheme 1 Synthesis of sensor **1**.

Fig. 7 The Benesi–Hildebrand plot of sensor **1** with Pb^{2+}. Linear equation: $Y = 5.09 \times 10^{-9} \times X + 1.04 \times 10^{-5}$, $R^2 = 0.9973$, $K_a = 2043$ M^{-1}.
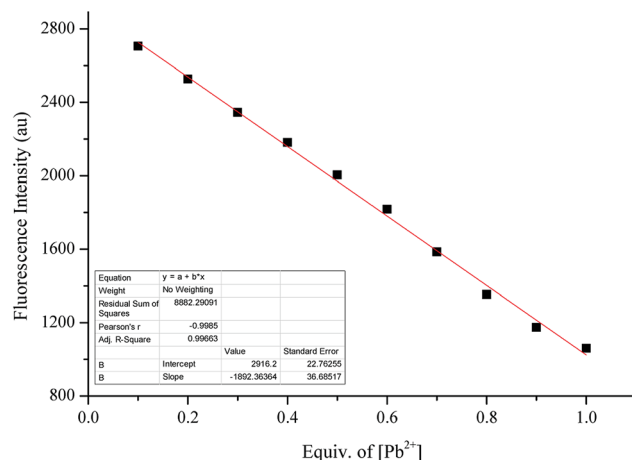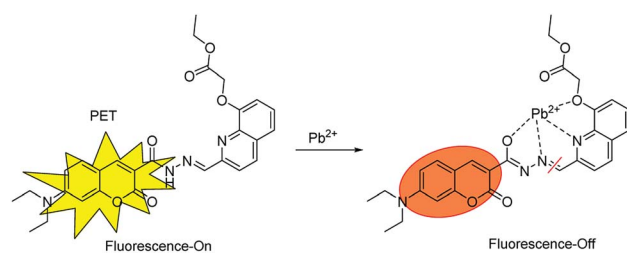

Fig. 8 The plot of the intensity at 485 nm for a mixture of sensor **1** and Pb^{2+} in CH_3CN/HEPES (9 : 1, v/v) buffer (pH = 7.4) in the range 0.1–1 equiv. ($\lambda_{ex} = 440$ nm). The calculated detection limit of **1** is 5×10^{-7} M.

Scheme 2 The possible mechanism of sensor **1** with Pb^{2+}.

the PET mechanism. In addition, the Job's plots indicated that sensors **1** chelated Pb^{2+} with 1 : 1 stoichiometry, as illustrated in Scheme 2, the addition of Pb^{2+} ion caused obvious fluorescence quenching and a color change from bright yellow to orange.

Conclusions

In this study, we have successfully prepared a fluorescence chemosensor **1** with coumarin as the fluorescence group and C=N bond and quinoline as the identification group. The pH test showed that the optimal pH range was from 4 to 8, indicating that sensor **1** could be used under acid and neutral conditions and *in vivo* cell tests. The absorption spectra showed no remarkable changes upon the addition of 10 equiv. of different metal ions, except that the addition of Pb^{2+} resulted in a red shift of 440 nm to 465 nm and a color change from bright yellow to orange. The fluorescence spectra showed an obvious quenching response to Pb^{2+} with a quenching efficiency of 99%. The Job plots showed that sensor **1** formed a 1 : 1 binding stoichiometry to Pb^{2+}, and the detection limit was 1.9×10^{-6} M, indicating high sensitivity of sensor **1** for Pb^{2+}. In addition, sensor **1** can be used for naked eye detection of Pb^{2+}, which can greatly broaden its applications.

Conflicts of interest

There are no conflicts to declare.

Acknowledgements

Notes and references

1 Z. Q. Zhang, X. W. He, Y. J. Shang, Z. Y. Yu, S. F. Wang and F. L. Wu, *Chem. Res. Chin. Univ.*, 2017, **33**, 31–35.

2 S. Goswami, A. Manna, K. Aich and S. Paul, *Chem. Lett.*, 2012, **41**, 1600–1602.

3 Y. Yu, W. Dou, X. Hu, X. L. Tang, X. Y. Zhou and W. S. Liu, *J. Fluoresc.*, 2012, **22**, 1547–1553.

4 F. Zapata, A. Caballero, A. Espinosa, A. Tárraga and P. Molina, *Org. Lett.*, 2007, **9**, 2385–2388.

5 O. Sunnapu, N. G. Kotla, B. Maddiboyina, S. Singaravadivel and G. Sivaraman, *RSC Adv.*, 2016, **6**, 656–660.

6 M. Alfonso, A. Tárraga and P. Molina, *J. Org. Chem.*, 2011, **76**, 939–947.

7 K. A. Hall, L. Jiang and R. K. Marcus, *J. Anal. At. Spectrom.*, 2017, **32**, 2463–2468.

8 M. Corte Rodríguez, R. Álvarez-Fernández García, E. Blanco, J. Bettmer and M. Montes-Bayón, *Anal. Chem.*, 2017, **89**, 11491–11497.

9 Z. Liu, Z. Zhu, H. Zheng and S. Hu, *Anal. Chem.*, 2012, **84**, 10170–10174.

10 M. Resano, M. Aramendía and M. A. Belarra, *J. Anal. At. Spectrom.*, 2014, **29**, 2229–2250.

11 T. Sun, Q. F. Niu, Z. R. Guo and T. D. Li, *Tetrahedron Lett.*, 2017, **58**, 252–256.

12 J. H. Bi, M. X. Fang, J. B. Wang, S. Xia, Y. B. Zhang, J. T. Zhang, G. Vegesna, S. W. Zhang, M. Tanasova, F. T. Luo and H. Y. Liu, *Inorg. Chim. Acta*, 2017, **468**, 140–145.

13 S. Samanta, B. K. Datta, M. Boral, A. Nandan and G. Das, *Analyst*, 2016, **141**, 4388–4393.

14 M. Devi, A. Dhir and C. P. Pradeep, *RSC Adv.*, 2016, **6**, 112728–112736.

15 Y. Zhang, W. Chen, X. Dong, H. Fan, X. Wang and L. Bian, *Sens. Actuators, B*, 2018, **261**, 58–65.

16 Z. Zhang, S. Lu, C. Sha and D. Xu, *Sens. Actuators, B*, 2015, **208**, 258–266.

17 W. Su, S. Yuan and E. Wang, *J. Fluoresc.*, 2017, **27**, 1871–1875.

18 Z. Q. Hu, C. S. Lin, X. M. Wang, L. Ding, C. L. Cui, S. F. Liu and H. Y. Lu, *Chem. Commun.*, 2010, **46**, 3765–3767.

19 L. L. Liang, F. F. Lan, S. G. Ge, J. H. Yu, N. Ren and M. Yan, *Anal. Chem.*, 2017, **89**, 3597–3605.

20 Shaily, A. Kumar, I. Parveen and N. Ahmed, *Luminescence*, 2018, **33**, 713–721.

21 M. W. Wang, F. Wang, Y. Wang, W. Zhang and X. Q. Chen, *Dyes Pigm.*, 2015, **120**, 307–313.

22 K. P. Nandre, A. L. Puyad, S. V. Bhosale and S. V. Bhosale, *Talanta*, 2014, **130**, 103–107.

23 F. Zapata, A. Caballero, A. Espinosa, A. Tárraga and P. Molina, *J. Org. Chem.*, 2009, **74**, 4787–4796.

24 E. Bardez, I. Devol, B. Larrey and B. Valeur, *J. Phys. Chem. B*, 1997, **101**, 7786–7793.

25 V. A. Montes, R. Pohl, J. Shinar and P. Anzenbacher Jr, *Chem.–Eur. J.*, 2006, **12**, 4523–4535.

26 K. G. Vaswani and M. D. Keränen, *Inorg. Chem.*, 2009, **43**, 5797–5800.

27 Y. W. Duan, H. Y. Tang, Y. Guo, Z. K. Song, M. J. Peng and Y. Yan, *Chin. Chem. Lett.*, 2014, **25**, 1082–1086.

28 N. Roy, S. Nath, A. Dutta, P. Mondal, P. C. Paul and T. S. Singh, *RSC Adv.*, 2016, **6**, 63837–63847.

29 G. F. Wu, M. X. Li, J. J. Zhu, K. W. C. Lai, Q. X. Tong and F. Lu, *RSC Adv.*, 2016, **6**, 100696–100699.

30 M. M. Yu, R. L. Yuan, C. X. Shi, W. Zhou, L. H. Wei and Z. X. Li, *Dyes Pigm.*, 2013, **99**, 887–894.

31 Z. T. Xing, H. C. Wang, Y. X. Cheng, T. D. James and C. J. Zhu, *Chem.–Asian J.*, 2011, **6**, 3054–3058.